Article

Discovery Medicine 2023; 35(179): 1147–1159
https://doi.org/10.24976/Discov.Med.202335179.111

Downregulation of HS6ST2 Inhibits Cervical Cancer Cell Migration and Invasion *in Vivo* and *in Vitro*

Shanfeng Li[1,2], Haichuan Shen[2], Qingzhi Wan[2], Pinjing Chen[2], Chenggan Shu[3], Hongmei Wang[4], Weipei Zhu[1,*]

[1]Department of Gynecology and Obstetrics, The Second Affiliated Hospital of Soochow University, 215000 Suzhou, Jiangsu, China
[2]Department of Gynecology and Obstetrics, Lianyungang Maternal and Child Health Hospital, 222062 Lianyungang, Jiangsu, China
[3]Department of Gynecology and Obstetrics, Yancheng First Hospital, Affiliated Hospital of Nanjing University Medical School, 210008 Nanjing, Jiangsu, China
[4]Department of Oncology, The Affiliated Hospital of Xuzhou Medical University, 221004 Xuzhou, Jiangsu, China
*Correspondence: zwp333xx@126.com; shamen60120@163.com (Weipei Zhu)
Published: 1 December 2023

Background: Emerging evidence indicates the importance of heparan sulfate 6-O-sulfotransferase 2 (HS6ST2) in a number of developmental processes. Little is known regarding its biological function in regulating cervical cancer (CC) progression. In this study, we aim to explore the role of HS6ST2 in CC progression.

Methods: The transcriptome sequencing data of CC tissues from three databases, GSE64217, GSE138080, and GSE63514, was examined for genes with significant changes. The expression profile for HS6ST2 within CC tissue was then assessed through fluorescence quantitative PCR and immunohistochemistry and compared to data from patients with clinicopathological features. A multivariate survival analysis was performed using the COX regression. The real-time quantitative PCR assessed the HS6ST2 expression profile within CC cellular cultures. The results of knocking down HS6ST2, considering the proliferative activity and invasiveness of CC cultures *in vitro*, were detected through cell viability assay, clonogenic assessment, tumorsphere formation analysis, 3D invasion experiment and transwell assay. The impact of HS6ST2 knockdown in CC proliferation was also evaluated *in vivo* using a nude mice model.

Results: HS6ST2 was severely upregulated within CC tissues across the three explored databases (GSE64217, GSE138080, and GSE63514). Fluorescent quantitative PCR and immunohistochemistry experiments identified HS6ST2 as highly upregulated within patients CC tissues. Survival analysis taking into account the parameters of lymph node metastasis, Federation of Gynecology and Obstetrics (FIGO) stage, depth of invasion, pathological grade, and HS6ST2 expression level demonstrated that individuals with downregulated HS6ST2 exhibited considerably extended progression-free survival (PFS) and overall survival (OS) in comparison to upregulated HS6ST2 cases. According to the findings of COX univariate analysis, the parameters lymph node metastasis, FIGO stage, depth of invasion, pathological grade, and HS6ST2 expression level, all showed a statistically significant correlation with effect upon prognosis of CC patients. The FIGO stage, depth of invasion and expression level of HS6ST2 were identified as independent risk variables influencing CC case prognosis within subsequent COX multivariate analysis. Cell function experiments proved that HS6ST2 knockdown can considerably diminish the proliferative potential, stemness and invasive traits of CC cells. Tumor formation experiments in nude mice *in vivo* demonstrated that knocking down HS6ST2 can significantly thwart CC cellular proliferative properties within animal models.

Conclusions: The clinicopathological features and the survival time of the patients significantly correlate with the level of HS6ST2 expression in CC tissue samples.

Keywords: cervical cancer; HS6ST2; proliferation; invasion

Introduction

Cervical cancer (CC) constitutes a frequent gynecological condition, accounting for more than 50% of the reproductive system malignancies. Its incidence rate is second only after breast cancer, and its case fatality rate ranks first among female malignancies [1,2]. The exact cause of the condition remains currently unknown. However, it is widely believed that numerous factors, including the infection with high-risk human papillomavirus as the first cause, the environment, the smoking frequency, experiencing numerous pregnancies and births are related to CC [3,4]. Surgical patients usually have a good outcome. Clinical studies have confirmed that the five-year survival rate for early CC can be as high as 70%–90%. Therefore, early diagnosis and treatment of CC are very important for prolonging survival and improving prognosis [5–7]. Predominantly, the cases that are diagnosed fall into the mid-/end-phases due to the

lack of characteristic clinical symptoms in the early stages of CC. Therefore, early, effective, and accurate diagnosis remains vital. For diagnosis and prognosis of CC, identifying blood tumor markers such as carcinoembryonic antigen (CEA) and cancer antigen 125 (CA125) has proven to be a crucial supplementary indication [8,9]. However, the detection rate is low, hence finding additional serum indicators to identify and screen for CC is vital.

Heparan sulfate (HS) is a linear sulfated glycosaminoglycan widely found within the extracellular matrix and in the cell membranes. It interacts with many ligands, participating in various cellular functions, such as cell growth, differentiation, adhesion and migration. HS also contributes to tissue morphology during cell development [10,11]. Heparan sulfate 6-O-sulfotransferase (HS6ST) is also pivotal to numerous developmental stages. Three HS6ST genomic family members, *HS6ST1, HS6ST2*, and *HS6ST3*, express a type II transmembrane protein within Golgi bodies [12]. HS6ST can regulate signal transduction pathways of multiple-growth factor receptors and increase the synthesis of those, including the hepatocyte growth factor (HGF), vascular endothelial growth factor (VEGF) and fibroblast growth factor (FGF), together with their relevant receptors [13,14]. Through controlling cell proliferation and angiogenesis, such growth factors have a crucial role in the development and progression of malignant tumors.

A recent study has found that HS6ST1 deficiency causes self-limited premature puberty in humans, compared to other gonadotropin-releasing hormone (GnRH) deficient genes [15]. HS6ST1 is overexpressed in cancer-associated fibroblasts and inhibits cholangiocarcinoma progression [16]. Moreover, suppressing HS6ST3 inhibits breast cancer cell proliferation and development by decreasing insulin like growth factor 1 receptor (IGF1R) and activating XIAP associated factor 1 (XAF1) [17]. Further, HS6ST2 is associated with the onset and growth of several aggressive tumor cells. For instance, the lncRNA FAM83H-AS1 inhibits non-small cell lung cancer proliferation and metastasis via the modulation of the miR-545-3p/heparan sulfate 6-O-sulfotransferase 2 (HS6ST2) axis [18]. In gastric cancer tissues, HS6ST2 is considerably expressed. Since HS6ST2 strongly correlates with certain clinicopathological variables and disease prognosis, it is considered as a new gastric cancer biomarker [19]. Also, overexpression of HS6ST2 in colorectal cancer (CRC) tissue is frequently associated with a bad prognosis. The dataset outcomes presented in our study support the role of HS6ST2 as a potential biomarker for cervical cancer prognoses [20]. Therefore, it is speculated that HS6ST2 may be a detection marker with important application potential. To explore the effectiveness of HS6ST2 in the early diagnosis and prognosis assessment of CC, this study investigated HS6ST2 expression profiles within CC in tissue and serum samples.

Study Methodology

Clinical Data Collection

Between January 2018 and December 2019, the medical records of individuals with CC admitted to Lianyungang Maternal and Child Health Hospital were compiled. Tumor tissue samples were obtained by surgery performed on patients with cervical cancer. Normal cervical tissues were obtained from the patients who underwent surgery with uterine myoma only. The samples were immediately preserved in liquid nitrogen at –196 ℃ and analyzed using Western blot, fluorescence quantitative PCR or formalin fixation and immunohistochemistry. None of the patients received chemotherapy or radiotherapy before surgery. This study was approved by the ethics committee of Lianyungang Maternal and Child Health Hospital. We obtained consent to publish the results from the participants, legal parents or guardians. All procedures performed in this study involving human participants were in accordance with the Declaration of Helsinki (as revised in 2013).

The inclusion criteria followed the pathological CC diagnosis, in line with the "Guidelines for the Diagnosis and Treatment for CC (Fourth Edition)": all primary tumors, full medical records and follow-up data. The exclusion criteria comprehended preoperative radiotherapy, chemotherapy, and other anti-tumor treatments. Seventy-six patients with CC were selected based on conditions for inclusion and exclusion. The age range was 31–62, having a mean age of (47.24 ± 10.32) years.

Immunohistochemical Analysis

The paraffin-embedded tissue specimens were sliced at 4 μm with the use of a microtome, fully baked and stained by immunohistochemical streptavidin-perosidase (SP) (Solarbio, Beijing, China), in order to identify HS6ST2 expression within CC tissues, cervical epithelial lesion tissue and normal cervical tissues. All operations were performed under the manufacturer's instructions. The rabbit anti-human HS6ST2 polyclonal antibody was obtained from the R&D Company (ab122220, Abcam, Cambridge, UK). The primary antibody was used at a working dilution of 1:200, while phosphate-buffered saline (PBS, PYJC059-2, Shanghai Shenqi Biotechnology Co., Ltd., Shanghai, China) served as negative control. The tissue specimens were stained with Diaminobenzidine (DAB, T15132, Shanghai Shangbao Biotechnology Co., Ltd., Shanghai, China), counterstained with hematoxylin, and then differentiated.

Semi-quantitative analysis was conducted taking into account the stain intensity of the cells and the positive cell population. Five high-power fields of view were randomly selected for scoring: (1) Score based upon degree of cell staining, 1 point for yellow or yellow-brown cells, 2 points for yellow-brown cells, and 0 points for no staining; (2) Rank dependent upon positive-cell degree: positive cells

under 5% score 0 points, those between 5% and 25% are rated 1; those between 26% and 50% are valued 2; and those beyond 50% are considered 3. The final score is determined by multiplying the two scores collectively. If the score is $\geq$2, it is set as positive (+); if $<$2, it is judged as negative (–); if the score is $\geq$3, it is denoted as high expression; and if it is $<$3, it is indicated as a low expression. The final scores were divided into low expression (0–5) and high expression ($>$5).

Fluorescence Quantitative PCR

After using RT-qPCR to determine the level of HS6ST2 expression in the tissue, total RNA was extracted using a Trizol RNA extraction kit (Sigma Company, St. Louis, MO, USA). First-strand cDNA was synthesized from 1 µg of RNA using the avian myeloblastosis virus (AMV) reverse transcriptase XL (Sangon Bioengineering Co., Ltd., Shanghai, China). For quantitative PCR analysis, reactions were run in the Bio-Rad iCycler equipment in the presence of SYBR Green dye (Invitrogen Life Technologies, Carlsbad, CA, USA). The primers used were the following:

HS6ST2 primer: Forward, 5′-GCCAACAACCGCCAAGTTC-3′; Reverse, 5′-AACGCCATGTGCTTCAGATTG-3′; *GAPDH* primer: Forward, 5′-CGTCCCGTAGACAAAATGGTGA-3′; Reverse: 5′-CCACTTTGCCACTGCAAATGG-3′.

An RT-PCR kit (Sigma Company, St. Louis, MO, USA) was used to determine the relative expression of HS6ST2. All procedures were followed according to the manufacturer's instructions. Finally, the $2^{-\Delta\Delta CT}$ formula was employed to determine the HS6ST2 expression-profile.

Cell Culture and Transfection

In order to measure the mRNA expression of HS6ST2 in CC cells, the cell cDNA chip (Shanghai, China) for HeLa, Ms751, Caski, C33A and SiHa, was purchased from Shanghai Outdo Biotech Co., Ltd. (Shanghai, China). The results showed that HS6ST2 was highly expressed in CC SiHa cells. SiHa cells (catalog number: TCHu113) were purchased from the National Collection of Authenticated Cell Cultures (Shanghai, China) and cultured in complete DMEM (PYJC338-3, Shanghai Shenqi Biotechnology Co., Ltd., Shanghai, China) carrying 10% FBS (FSP500, Shanghai Exel Biotech, Shanghai, China) and 5% CO_2 at 37 °C. We tested the cell cultures for mycoplasma using the Applied Biosystems MycoSEQ detection kit (Thermo Scientific, Rockford, IL, USA); the results were negative. On the other side, short tandem repeat (STR) identification was confirmed by Wuhan Zhishan Biotech Co., Ltd. (Wuhan, China) on August 5th, 2022.

For the transfection, cultures within the logarithmic growth phase were inoculated into 6-well plates at a confluence of 2×10^5 cells/mL and transfected once they reached 70% confluency, then placed at a controlled temperature for culturing and 5% CO_2 at 37 °C. They were constantly grown for 6 h in an incubator, replaced with a complete cell culture medium and continued to grow for 48 h. Transfection efficiency was tested and subsequent experimental analysis was carried out. Specific Sh-RNAs against HS6ST2 (Sh-RNA1 (5′-UCACGGCAAAUAGGAAGAG-3′), Sh-RNA2 (5′-CGACUACAUAGGCAGUGUA-3′)) and their corresponding Sh-RNA-Normal Control (Sh-NC) were bought from GenePharma (Shanghai, China).

CCK-8 Detects Cell Viability

Transfected cultures were seeded within 96-well plates, 2×10^3 cells per well and three replicates per cohort. Cells were grown for 12, 24, 36 and 48 hours. Ten µL of cell counting kit-8 (CCK-8) reagent (Beyotime, Beijing, China) were set, followed by incubation for 120 minutes. Then the optical density (OD) value was determined at 490 nm through a microplate reader. The assessment was performed on three separate occasions and the average was determined.

Clonogenic Assessment

Transfected cells were inoculated within a 6-well plate, 600 cells per well, with medium replaced at 72-h intervals. After 14 days of growth, cultures were fixed through 1 mL 4% paraformaldehyde (203-812-5, Nanjing Chemical Reagent Co., Ltd., Nanjing, China) for 30 minutes and thrice-rinsed using PBS, with subsequent introduction within each well. Cells were stained with 1 mL 1% crystal violet staining solution (CD434595, Guangzhou Hewei Medical Technology Co., Ltd., Guangzhou, China) for 10 minutes and thrice rinsed using PBS. Colonies were counted three times and the average was obtained.

Tumorsphere Formation

After the transfected cells were digested and centrifuged, they were set into a single-cell suspension and counted. Then, 500 cells were placed in an ultra-low adsorption culture dish, serum-free medium containing 20 ng/mL of bFGF, 20 ng/mL EGF and 2% B27 growth factors (ScienCell, Carlsbad, CA, USA). After 7 days of culture, spherical cell clusters were observed under the microscope and dataset outcomes were recorded.

3D Spheroid Cell Invasion Assessment

A 3D spheroid cell invasion assessment kit was obtained by Trevigen™ (Bio-Techne, Minneapolis, MN, USA). Assays were performed following the manufacturer's instructions. Spheroids were imaged within individual well at daily intervals. The spheroid area was determined through Image J (version 1.8.0, National Institute of Health, Bethesda, MD, USA).

Fig. 1. Screening of considerably different genes in cervical cancer (CC) tissue. The absolute value of log fold change >2, and the *p* value < 0.02.

Transwell Assay

Matrigel (BD Biosciences, Bedford, MA, USA) was thawed and diluted through serum-free DMEM medium in a 1:8 proportion; evenly coated upon microporous membrane for transwell chamber (8 µm-pore sizes, Corning, New York, USA) and placed into incubation at 37 °C per 120 minutes. Individual cellular cohorts were converted into suspensions comprising 1×10^4 cells/mL with serum-free medium, followed by 100 µL cell suspension being seeded within the upper section of the transwell chamber and 700 µL complete cell culture medium introduced within the lower chamber. Cells were cultured for 48 h. After taking out the small chamber, cells from the upper layer of the microporous membrane were carefully cleansed through cotton swabbing; washed with PBS twice and fixed with 95% ethanol. Then they were stained with 1% crystal violet solution; rinsed with PBS; observed under an inverted microscope and counted. The mean value of 6 fields per view for each group was utilized.

Western Blotting

Total proteomic cellular content was collected through RIPA. Proteins were determined through the BCA technique, and 10% Sodium dodecyl sulfate-polyacrylamide gel (SDS-PAGE) (R21149, Shanghai Yuanye Biotechnology Co., Ltd., Shanghai, China) electrophoresis gel was run. After the run, the membrane was transferred and blocked, and then diluted 1:800 with HS6ST2 (ab122220, Abcam, Cambridge, UK) and 1:1000 with glyceraldehyde-3-phosphate dehydrogenase (GAPDH) (ab9485, Abcam, Cambridge, UK) primary antibodies. Membranes were incubated overnight in a refrigerator at 4 °C, then the membrane was washed, and horseradish peroxidase-labeled (9003-99-0, Wei Shi Chemical Reagent Co., Ltd., Wuhan, Hubei, China) secondary antibody immunoglobulin G (IgG) at 1:2000 dilution (AS014, Abclonal, Wuhan, Hubei, China) was set in a shaker at 37 °C for 60 minutes. Enhanced chemiluminescence (ECL) (ECL-F-100, Yanxi Biotechnology Co., Ltd., Shanghai, China) reagent was added in the dark, and pictures with gel imaging system exposure were taken.

In Vivo Nude Mouse Experiments

Hepatoma cells that overexpress TINCR ubiquitin domain containing (TINCR) and their control cells (1×10^6) were mixed with Matrigel™ and injected subcutaneously within the abdomens of mice (nod/scid, Saiye Biotechnology Co., Ltd., Guangzhou, Guangdong, China) aged 8–12 weeks. Measurement was done once a week for five weeks after the tumor formation. The formula employed for calculating the tumor volume was: $V = 1/2 \times a \times b^2$ (a = long axis; b = short axis). Tumor growth curves were designed based on the obtained data. Mice were placed in a new cage with corn cob bedding, and immediately euthanized by displacement of air with 100% carbon dioxide (124-38-9, Kedian Gas Chemical Co., Ltd., Foshan, China) for 5 min. Then the tumors were dissected and weighed.

Statistical Analysis

SPSS 20.0 (IBM SPSS statistics, Chicago, IL, USA) was used to analyze the data. A chi-square test was employed to calculate the positive rate of HS6ST2 protein in various cervical tissues. The correlation between the expression of HS6ST2 in patients with CC and clinicopathological data was assessed. Overall survival (OS) and disease-free survival (DFS) rates were analyzed by Kaplan–Meier analysis and Log-rank statistical test. Univariate and COX multivariate regression algorithms were performed to establish the independent prognostic factors for DFS and OS. The hazard ratio (HR) with a 95% confidence inter-

val (CI) was used to represent relative risk in COX multivariate analysis. Student's *t*-test was utilized to analyze the significant differences between the two groups, while analysis of variance (ANOVA) was used to examine statistical differences among multiple groups. The diagnostic potential of the HS6ST2 protein was examined using the receiver operating characteristic curve (ROC). Student's *t*-test was used to evaluate the differences between variables, and the *p* value less than 0.05 was considered as statistically significant.

Results

HS6ST2 Expression in CC Tissues

First, we downloaded the published transcriptome sequencing data from CC tissues (GSE64217, GSE138080, and GSE63514). The screening criteria were: log fold change absolute value >2 and *p* value < 0.02. Then we took the intersection of the three datasets and found five common genes: *KLHDC7B*, *CDKN2A*, *APOC1*, *HS6ST2* and *AIM2* (Fig. 1).

Additional examination of the five genes, as mentioned above, revealed the following: Heparan sulfate 6-O-sulfotransferase 2 (HS6ST2) and Apolipoprotein C1, also known as apolipoprotein C1 (APOC1) are two related enzymes. Absent in Melanoma-2, AIM2 is the missing protein 2 in melanoma, and the Cyclin-dependent Kinase Inhibitor 2A (CDKN2A) is a cyclin-dependent kinase inhibitor as their names indicates. Among these, HS6ST2 is primarily found within the cytoplasm, the extracellular matrix and the basement membrane. Through interactions with different proteins or ligands, it affects physiological activities including cellular development, differentiation, adhesion, and migration [11,13,14]. In contrast, the other four proteins are mostly found in the cytoplasm and the nucleus. We speculate that HS6ST2 may be shed from the cell surface, in which case the protein level can be detected in the blood to predict or evaluate tumor progression. HS6ST2 was selected for research in follow-up studies.

Expression of HS6ST2 in CC Tissues

We acquired 14 cases of CC tissue and 14 cases of paracancerous tissue within the early stages of the disease. The RNA and protein were extracted, and HS6ST2 expression was determined by fluorescence quantitative PCR and Western blot in order to validate the outcomes of the preceding analysis. HS6ST2 was upregulated within 71.4% (10/14) of the cancerous tissues among the 14 matched paracancerous, and it was elevated by 21.4% (3/14) in the cancerous tissues from the para-tumoral tissues. 7.1% (1/14) of cancer tissues exhibited lower expression of HS6ST2 levels than that of the paracancerous (Fig. 2). In summary, the mRNA level of HS6ST2 within CC tissues was substantially upregulated, compared to the paracancerous tissues.

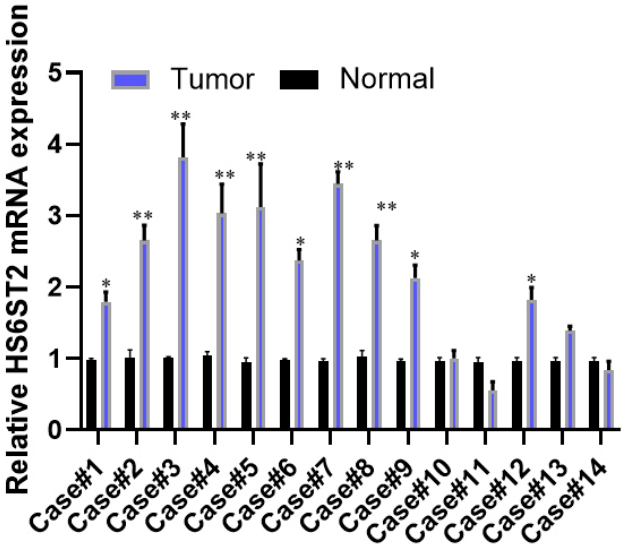

Fig. 2. Fluorescent quantitative PCR detection of heparan sulfate 6-O-sulfotransferase 2 (HS6ST2) mRNA expression in 14 cases of CC and neighbouring tissues. Data are presented as means ± SD of three independent experiments (n = 3). *$p < 0.05$ vs Normal, **$p < 0.01$ vs Normal.

Using immunohistochemistry, as presented in Fig. 3A,B, the expression of HS6ST2 in human CC tissues was determined to be higher than that in adjacent non-tumor tissues.

An Examination of the Relationship between HS6ST2 Expression Levels in CC Tissues and Patient Clinical Status

The clinical information of CC patients was gathered, and the association between the clinicopathological characteristics of individuals and HS6ST2 expression was calculated. Investigational findings demonstrated that HS6ST2 expression was strongly associated with pathological grade, Federation of Gynecology and Obstetrics (FIGO) stage, and lymph node metastases but not with age, tumor diameter, the extent of invasion, or the histological type in CC patients (all $p < 0.05$, Table 1).

The Association between Plasma HS6ST2 Expression Levels and CC Patients' Prognosis

According to dataset outcomes of immunohistochemistry, overall survival (OS) and progression-free survival (PFS) curves for cases of high HS6ST2 expression (n = 50) and progenitors having low HS6ST2 expression (n = 26) were constructed. The findings highlighted that individuals with downregulated HS6ST2 exhibited substantially longer PFS and OS compared to those with upregulated HS6ST2 ($p = 0.017$ and $p = 0.034$, Fig. 4A,B).

Table 1. Association between HS6ST2 expression levels within CC tissues and patient clinical pathological profiles.

Clinical pathological features	No. of patients (n = 76)	HS6ST2 High expression (n = 50)	HS6ST2 Low expression (n = 26)	χ^2	p
Age (Years)				0.6652	0.4147
<45	36	22	14		
≥45	40	28	12		
Lymph node metastasis				3.939	*0.0472
Yes	44	33	11		
No	32	17	15		
Tumor diameter				1.726	0.1890
<3 cm	51	31	20		
≥3 cm	25	19	6		
FIGO stage				7.577	*0.0059
I	36	18	18		
II	40	32	8		
Infiltration				1.949	0.1627
≤1/2 myometrium	27	15	12		
>1/2 myometrium	49	35	14		
Pathological grade				7.605	*0.0058
G1+G2	45	24	21		
G3	31	26	5		
Histological type				1.949	0.1627
Adenocarcinoma	19	10	9		
Squamous cell carcinoma	57	40	17		

*significant value.

FIGO, Federation of Gynecology and Obstetrics.

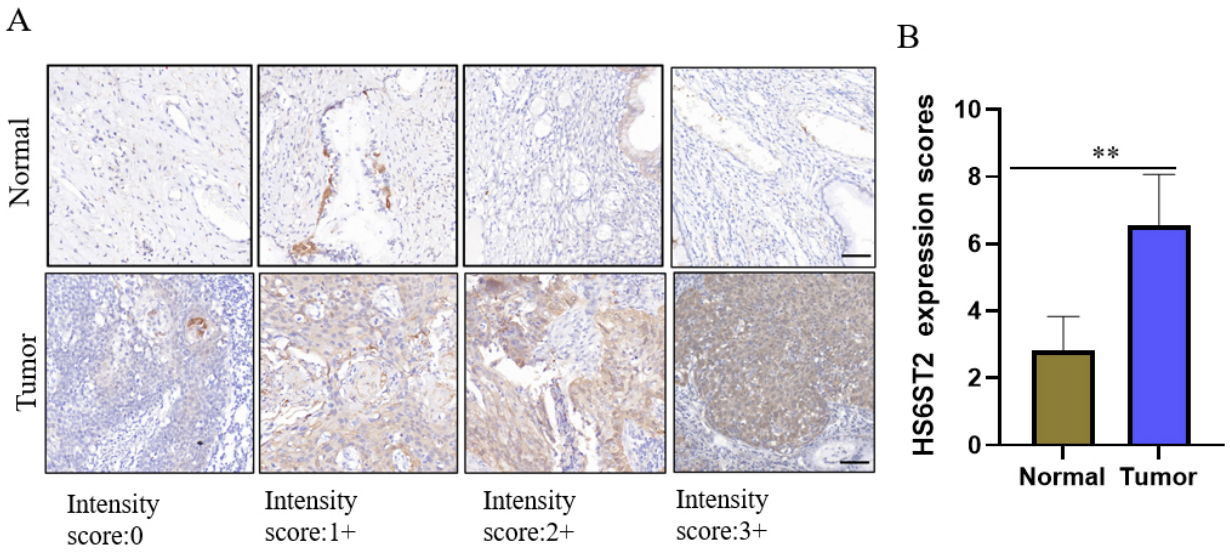

Fig. 3. Analysis of the immunohistochemical expression of HS6ST2 in CC tissues. (A) Representative images of immunohistochemistry (IHC) staining with anti-HS6ST2 antibody from CC and adjacent cervical epithelial tissues in a human microarray. (B) Scores of IHC staining are represented. Scale bar = 100 µm. **$p < 0.01$.

COX Univariate and Multivariate Analysis Affecting the Diagnosis of Individuals with CC

The variables influencing the prognosis of patients with CC were investigated using clinicopathological data from the patients and 5-year OS data from follow-ups. The findings of the COX univariate analysis revealed that the depth of invasion, lymph node metastasis, FIGO stage and pathological grade, together with HS6ST2 expression level, influenced the CC patient's prognosis ($p < 0.05$, Table 2). Further, COX multivariate analysis results revealed

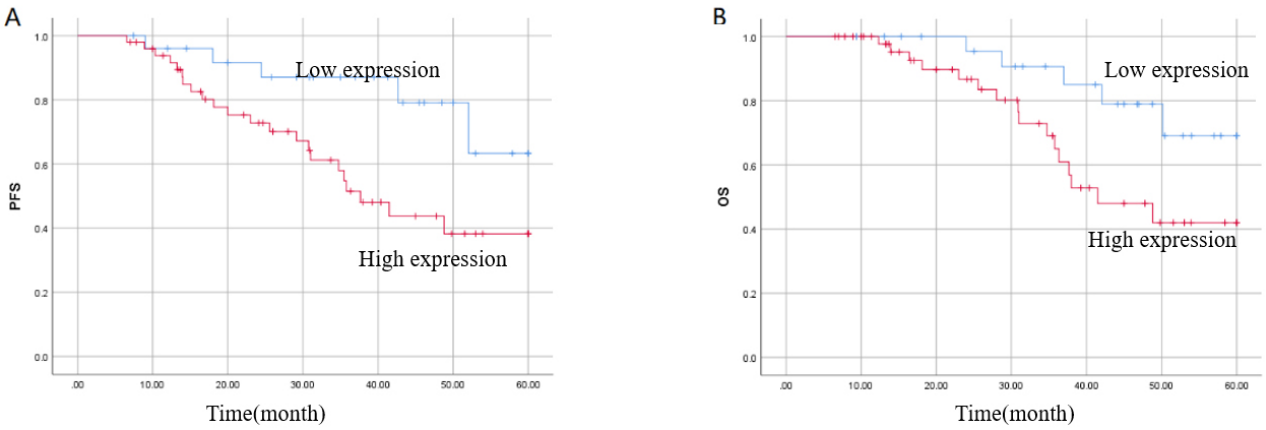

Fig. 4. An evaluation for progression-free survival (PFS) (A) and overall survival (OS) (B) across cases of varying levels of HS6ST2 expression.

Table 2. COX univariate assessment affects the prognosis of CC patients.

Clinical pathological feature	B	SE	*p*	Exp (B)	95% Exp (B) for CI	
					Lower limit	Upper limit
Age	–0.705	0.454	0.121	0.494	0.203	1.203
Lymph metastasis	1.636	0.628	0.009	5.137	1.500	17.588
Tumor diameters	0.063	0.484	0.897	1.065	0.413	2.747
FIGO staging	3.031	1.026	0.003	20.714	2.775	154.597
Infiltration depth	2.513	1.025	0.014	12.244	1.655	9.069
Pathological grade	1.939	0.515	0.000	6.955	2.535	19.083
Histological type	0.494	0.513	0.336	1.639	0.599	4.480
HS6ST2 expression	2.821	1.026	0.006	16.791	2.249	125.337

Table 3. COX multivariate analysis and prognosis of CC patients.

Clinical pathological feature	B	SE	*p*	Exp (B)	95% Exp (B) for CI	
					Lower limit	Lower limit
Lymph metastasis	1.444	0.660	0.029	4.236	1.163	15.431
FIGO staging	2.138	1.081	0.048	8.479	1.020	70.502
Infiltration depth	1.425	1.114	0.201	4.160	0.469	36.913
Pathological grade	0.550	0.569	0.334	1.732	0.568	5.286
HS6ST2 expression	1.528	1.247	0.045	6.867	1.423	56.016

that FIGO stage, lymph metastasis and HS6ST2 expression level were independent risk factors affecting CC prognosis ($p < 0.05$, Table 3).

In addition, according to the published CC transcriptome data in the TCGA database (http://gepia.cancer-pku.cn/index.html), further analysis found that HS6ST2 was overexpressed in CC tissue (Tumor) than in the paracancerous tissue (Fig. 5A). The study discovered that patients with high HS6ST2 expression exhibited considerably longer survival than individuals with low expression (Fig. 5B). The dataset outcomes mentioned previously suggested that the expression level of HS6ST2 could be exploited as a possible detection marker for the prognosis of CC.

Further examination of the patient's survival period based on pathological characteristics for CC patients, M0 in the M stage, N1 in the N stage, Squamous cell carcinoma, clinical grade in the patient, T1 grading stages I and T. OS of CC individuals with high HS6ST2 expression was demonstrated to be considerably shorter compared to cases with low expression of the marker (Fig. 6).

HS6ST2 is Highly Expressed within CC Cell Lines and Regulates Cellular Proliferation/Stemness

Such above experimental results show that the expression level of HS6ST2 has a major association with the clinical characteristics and survival period of CC patients. Consequently, further exploration of HS6ST2 influence regarding the malignant biological behavior of CC cells was performed. First, HS6ST2 expression within CC cells was determined through fluorescent quantitative PCR. Dataset outcomes demonstrated that, in comparison to cervical ep-

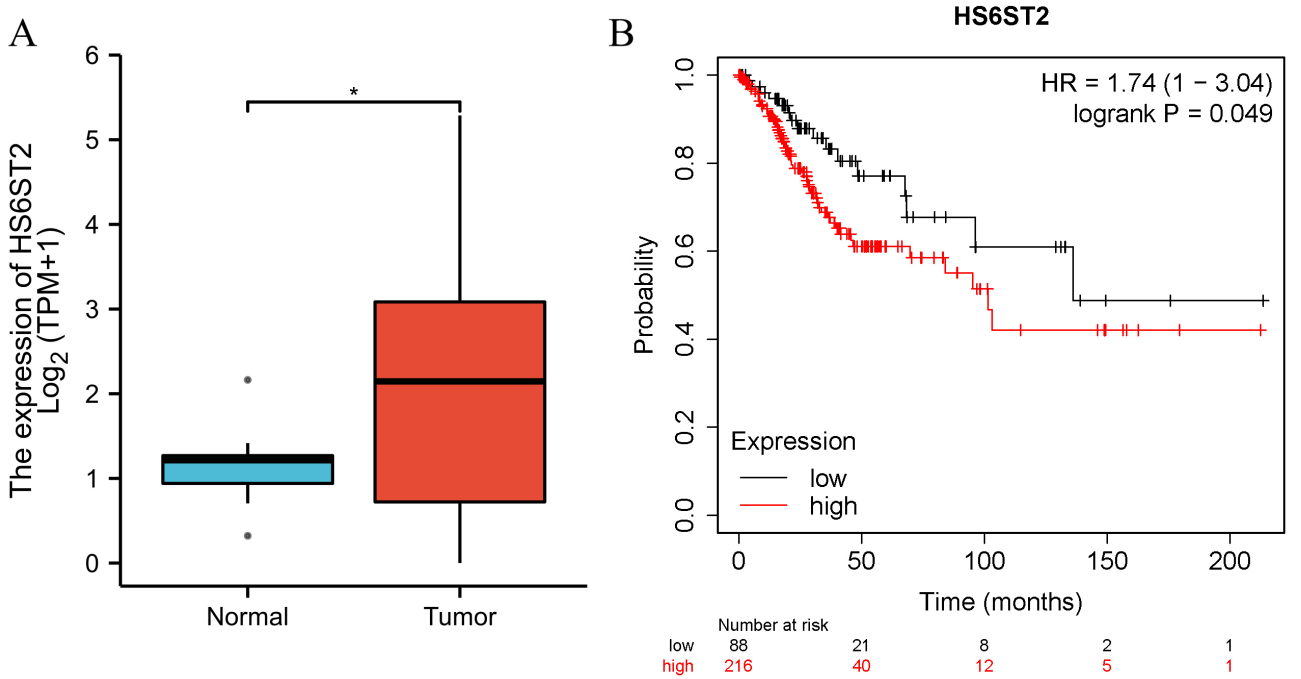

Fig. 5. HS6ST2 was overexpressed in CC tissue. (A) TCGA database analysis of HS6ST2 expression in CC tissues, *$p < 0.05$ vs Normal. (B) TCGA database analysis impact by HS6ST2 expression on patient OS. HR, hazard ratio.

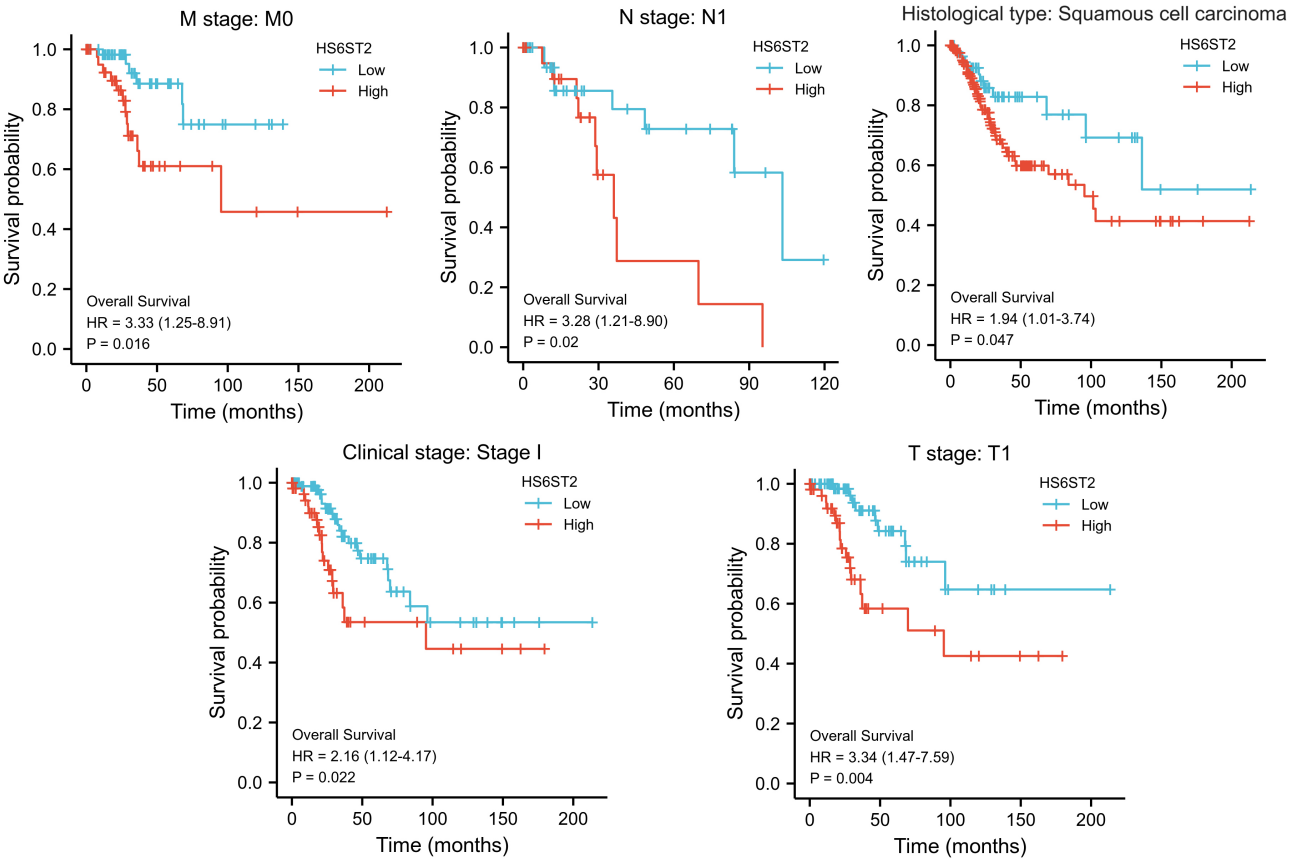

Fig. 6. Correlation of HS6ST2 expression from TCGA data with OS in clinicopathological subgroups of CC patients.

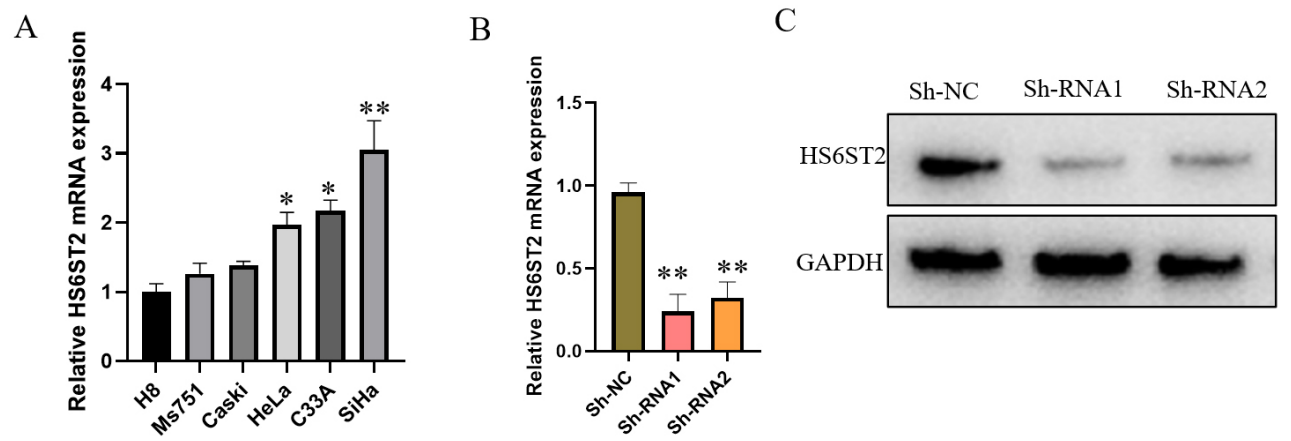

Fig. 7. HS6ST2 level within CC cultures. (A) RT-qPCR assessment for HS6ST2 transcriptomic expression within CC cultures. (B) RT-qPCR assessment for HS6ST2 transcriptomic expression within CC cultures post-transfection/knockdown of HS6ST2 vector mRNA expression. (C) Western blot detection for HS6ST2 proteomic expression within CC cells after transfection knockdown HS6ST2 vector. Data are presented as means ± SD of three independent experiments. GAPDH, glyceraldehyde-3-phosphate dehydrogenase. *$p < 0.05$ vs Cervical epithelial immortalized cells (H8), **$p < 0.01$ vs H8 or Sh-RNA-Normal Control (Sh-NC).

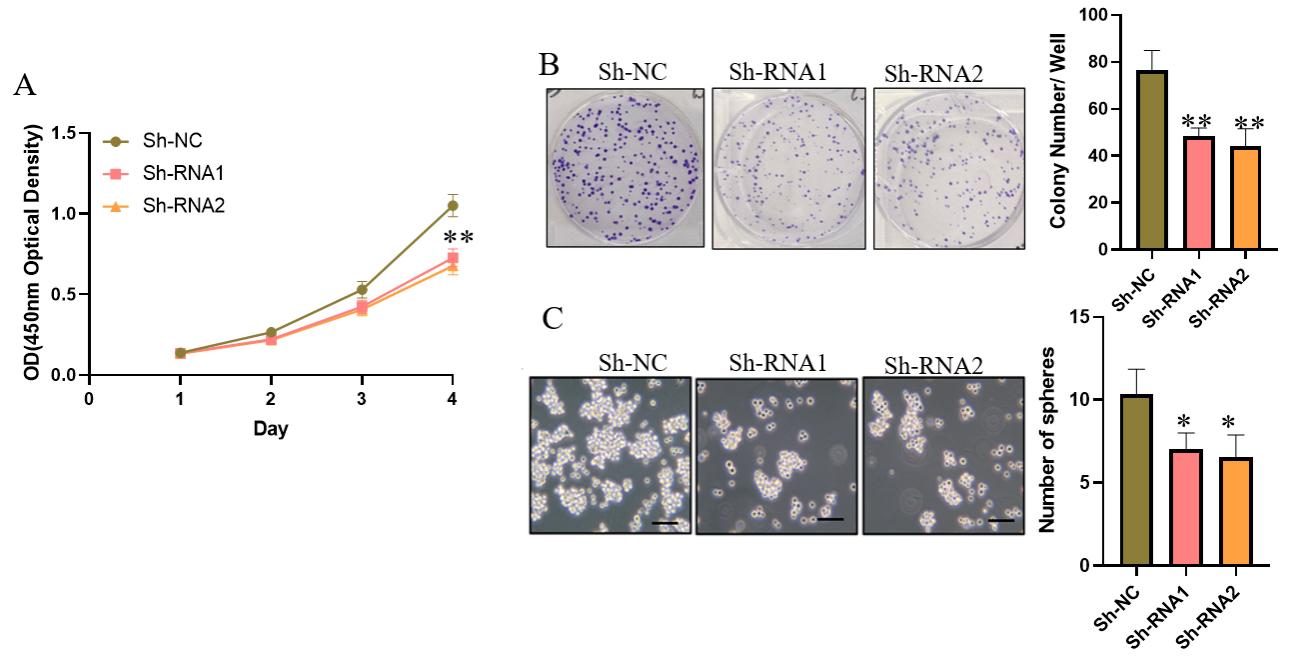

Fig. 8. Impact of HS6ST2 knockdown upon viability, proliferation and stemness of CC cells. (A) Cell counting kit-8 (CCK-8) identifies the impact by knocking down HS6ST2 upon cell viability. (B) Plate colony formation assessment exposes the impact of HS6ST2 downregulation on cell viability. (C) Spheroid culture after HS6ST2 knockdown on cellular stemness. Data are presented as means ± SD of three independent experiments. Scale bar = 50 µm, *$p < 0.05$ vs Sh-NC, **$p < 0.01$ vs Sh-NC.

ithelial immortalized cells (H8), HS6ST2 was highly expressed within the CC cells lines (HeLa, C33A, SiHa), Ms751 and Caski cells (Fig. 7A). Next, the design and synthesis of lentiviral short hairpin RNA (Sh-RNA1 and Sh-RNA2), targeting different sequences of HS6ST2 and the blank control vector Sh-NC were performed. Then SiHa cells were transfected with high expression of HS6ST2 Sh-RNAs, and knockout was detected by fluorescent quantitative PCR and Western blot, respectively. Dataset outcomes demonstrated that transfection of lentiviral Sh-RNA1 and Sh-RNA2 targeting different sequences of HS6ST2 could considerably reduce HS6ST2 mRNA and protein in SiHa cells, compared to blank control vector, Sh-NC ($p < 0.01$, Fig. 7B,C).

Next, the impact of HS6ST2 knockdown upon active proliferation and stem cell formation for CC cells were detected through CCK-8, clonogenic and tumorsphere assessment, respectively. Dataset outcomes for CCK-8 experi-

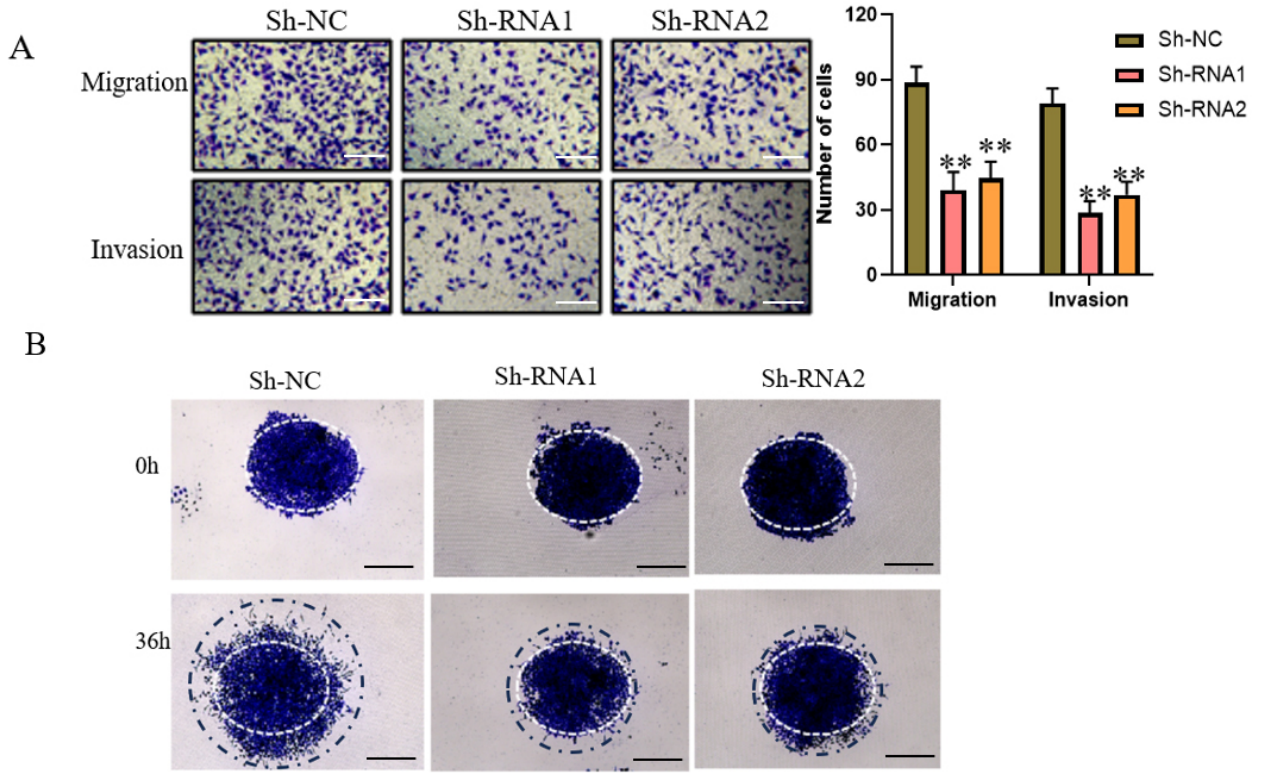

Fig. 9. Impact of Sh-RNA1 and Sh-RNA2 on CC cells migration and invasion. (A) Transwell assessment detected the impact of HS6ST2 knockdown in the migration and invasion of CC cells. (B) 3D cell migration assessment after HS6ST2 downregulation in CC cells effect on invasion. Data are presented as means ± SD of three independent experiments. Scale bar = 100 µm, $^{**}p < 0.01$ vs Sh-NC.

ments demonstrated that knockdown by Sh-RNA1 and Sh-RNA2 of HS6ST2 expression considerably inhibited cell viability in comparison to the blank control vector (Sh-NC) (Fig. 8A, $p < 0.05$). Plate colony formation dataset outcomes demonstrated that knockdown of HS6ST2 expression can severely thwart colony formation in comparison to Sh-NC (Fig. 8B, $p < 0.01$). Dataset outcomes of tumorsphere culture showed, that compared to Sh-NC, knockdown of HS6ST2 expression can considerably thwart the number and size of cell spheres (Fig. 8C, $p < 0.05$.). The above results indicated that the downregulation of HS6ST2 inhibited the viability, proliferation and stemness of CC cells.

Effect of HS6ST2 Knockdown Upon Migration and Invasion of CC Cells

Dataset outcomes of the transwell test demonstrated that compared to the Sh-NC condition, Sh-RNA1 and Sh-RNA2 could considerably inhibited the ability of CC cells to pass from the upper chamber of the transwell to the lower chamber (Fig. 9A, $p < 0.01$). At the same time, compared to Sh-NC, knockdown of HS6ST2 considerably inhibited the cells' capacity to invade from the upper chamber of transwell coated with matrigel to the lower chamber (Fig. 9A, $p < 0.01$). This impact on the invasion treats of the cells was further detected by 3D culture. First, the cells were mixed with matrigel, and then inoculated into 48 wells and cultured overnight, and then photographed at 0 h, and after a 36-h interval. The dataset outcomes demonstrated that cells in the blank control cohort began to migrate from the center to the periphery, while the number and extent of cells migrating to the periphery in the knockdown groups were considerably reduced (Fig. 9B). The above results indicated that knocking down HS6ST2 inhibited the migration and invasion of CC cells.

Knockdown of HS6ST2 Inhibited Tumor Growth in Vivo

Two groups of female nude mice, divided into five animals per group, were injected subcutaneously with HS6ST2-knockdown CC cells. The nude mice were sacrificed 35 days later. Dataset outcomes showed that, in comparison to Sh-NC, knockdown by Sh-RNA1 could considerably thwart the proliferation ability of the cells in nude mice (Fig. 10A). According to the growth curve, the growth rate of Sh-RNA1 HS6ST2 CC cells in nude mice was considerably lower than that of the control cohort (Fig. 10B, $p < 0.01$). The weight of tumor-bearing tissues was also significantly lower than that of the control cohort (Sh-NC) (Fig. 10C, $p < 0.01$). The above results indicated that knocking down HS6ST2 could greatly diminish the proliferation ability of CC cells.

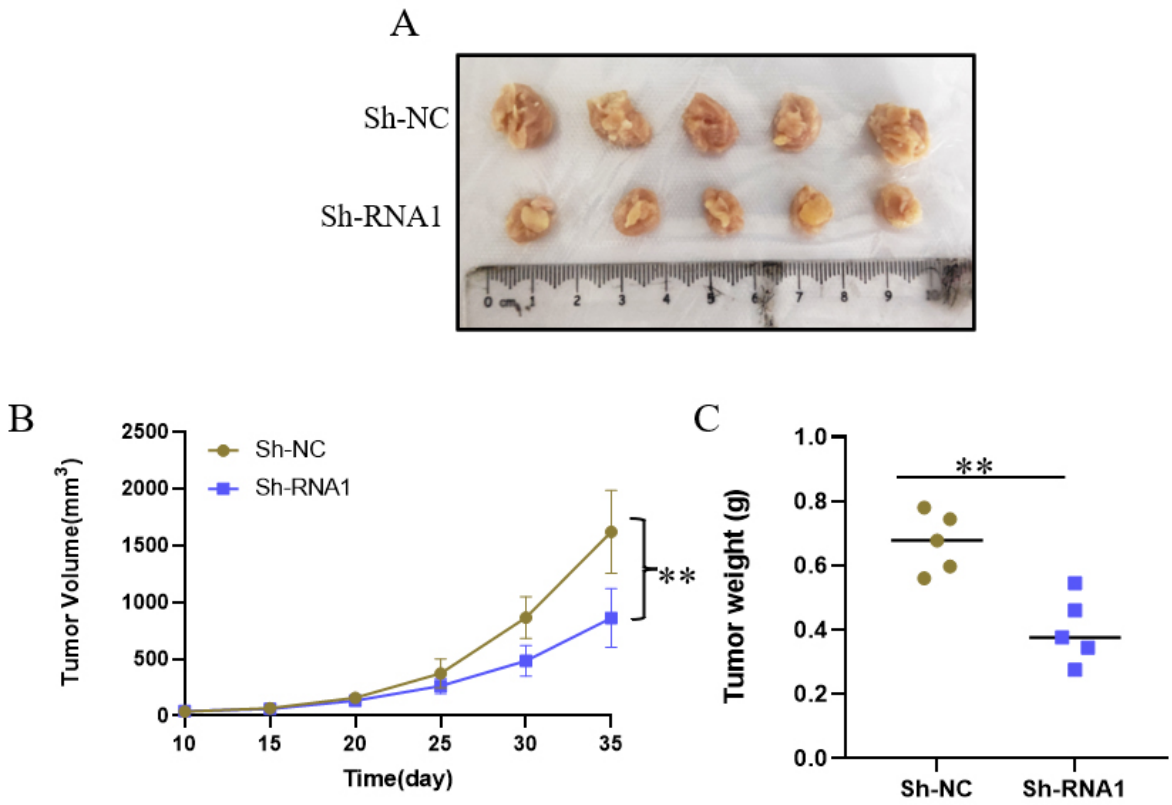

Fig. 10. HS6ST2 knockdown inhibited tumor growth *in vivo*. (A) The morphological characteristics of the tumor-bearing tissue formed 35 days after subcutaneous inoculation. (B) The volume change of the tumor-bearing tissue was monitored on the 10th day after inoculation. (C) The weight of the formed tumor-bearing tissue, $^{**}p < 0.01$ vs Sh-NC.

Discussion

The most prevalent aggressive tumor of the female reproductive system is CC, which arises from the cervix and cervical canal [21]. Diagnostic markers exhibiting high specificity and sensitivity are required since CC's early stages lack particular clinical signs, which increases the risk of missed or incorrect diagnoses. HS6ST2 was identified as being highly expressed in three CC datasets in this study by TCGA screening. Additionally, it was discovered, through clinical sample detection, that HS6ST2 was highly upregulated within CC tissue, having a strong association with clinicopathological profiles for lymph node metastases, FIGO stage, and pathological grade. The survival assessment demonstrated that individuals with low HS6ST2 expression exhibited significantly longer PFS and OS in comparison to those with high HS6ST2 expression.

According to the findings of COX univariate analysis, the prognosis of CC patients was affected by lymph node metastasis, FIGO stage, depth of invasion, pathological grade, and HS6ST2 expression level. FIGO stage, invasion depth, and HS6ST2 expression level were revealed to be risk factors influencing the prognosis of CC patients in a subsequent COX multivariate analysis. Additionally, functional experiments proved that knocking down HS6ST2 could considerably thwart the proliferation and invasion of CC cells. *In vivo* experiments further demonstrated that HS6ST2 downregulation could considerably thwart the *in vivo* proliferation of CC cells.

Three isoforms of the heparan sulfate 6-O-sulfotransferase (HS6ST) family—*HS6ST1*, *2*, and *3* are responsible for attaching sulfate to heparan sulfate proteoglycans (HSPGs) [22]. A member of the HS6ST family named HS6ST2, HS6ST-2s is an independently spliced version missing 40 amino acids. The sulfate cohort is transferred from 3'-phosphoadenosine, 5'-phosphophosphate (PAPS) to the 6-O position of the glucosamine residue in HSPGs by these two enzymes, despite their differing sequences [23]. Through interactions with several cytokines, HSPGs participate in several biological processes through this pathway, including coagulation, cell recognition, adhesion, proliferation, and differentiation [24]. HS6ST2 is overexpressed in malignant tumors, such as stomach, kidney, and lung, and strongly correlates with prognosis [18,19,25]. The main characteristic of tumor cells is to proliferate indefinitely despite regulation [26]. Therefore, dataset outcomes of this study showed that HS6ST2 is considerably upregulated within the CC cells HeLa, C33A,

and SiHa. By constructing CC cell lines with knocked HS6ST2, we were able to observe the HS6ST2 effect on the viability, proliferation and cell stemness. The dataset outcomes of this study are consistent with previous reports showing that HS6ST2 is involved in regulating energy metabolism and thyroid hormone levels in mice, thereby affecting growth and development [27]. Knocking down the expression of HS6ST1/2 in glioma tissue can considerably thwart the heparan sulfate biosynthesis system, thereby promoting the proliferation and invasion of glioma [28].

In addition, the prognosis of patients with metastatic CC is very poor, which is also the main factor leading to patients' death. There are two ways of the cervical cancer can metastasize, through the blood and the lymph. The mortality risk of patients with blood metastasis is higher than that of patients with lymphatic metastasis [29,30]. Studies have shown that oncogenes or tumor suppressor genes are involved in regulating the invasion and metastasis of CC cells. For example, knockdown of metastasis-associated 1, family member 2 (MTA2) can reduce the metastatic potential of CC cells by inhibiting the expression of matrix metalloproteinase 12 (MMP12) [31]. As a tumor suppressor, olfactomedin 4 (OLFM4) inhibits CC metastasis by regulating the mammalian target of rapamycin (mTOR) signaling pathway [32]. This study also proved that knocking down HS6ST2 can considerably diminish the metastasis and invasion ability of the cells, showed through transwell assay and 3D invasion experiments. Dataset outcomes of *in vivo* experiments further demonstrated that knocking down HS6ST2 could considerably decrease the proliferation ability of CC cells *in vivo*. In addition, studies have shown that HS6ST2 can also participate in the glycolysis process of tumor cells, and as a detection biomarker to predict patient survival [33]. HS6ST2 can affect the migration of hindbrain facial nerve neurons by regulating fibroblast growth factor (FGF) signaling [34]. In the Alzheimer's disease, the expression of heparan sulfate-glucosamine 3-sulfotransferase 2 (HS3ST2) is critical for the abnormal phosphorylation of the TAU protein [35]. Nevertheless, the precise role played by the HS6ST2 protein in the onset and progression of CC is presently unknown and requires additional studies. This protein might be connected to the increase in the growth factor signaling, which causes the aggressive development of CC cells.

Conclusions

The study findings revealed that the HS6ST2 protein can be employed as an auxiliary screening marker for CC detection. However, this needs further confirmation by extensive clinical trial data.

Availability of Data and Materials

All data in this study are available upon request by writing to the corresponding author.

Author Contributions

SFL and WPZ performed the acquisition, analysis, and interpretation of data. SFL and HCS analysis, interpretation of data and drafted the manuscript. QZW, PJC, and CGS provided technical, material support and revising the manuscript critically. HMW and WPZ conducted design, supervision and drafted the manuscript. All authors read and approved the final manuscript. All authors have participated sufficiently in the work and agreed to be accountable for all aspects of the work.

Ethics Approval and Consent to Participate

This study was approved by the Ethics Committee of Lianyungang Maternal and Child Health Hospital (2022-12-312) and was conducted in accordance with relevant guidelines and regulations. Written informed consent was obtained from each participant. The animal experiment was approved by the Ethics Committee of Lianyungang Maternal and Child Health Hospital (approval number: LYG-ME202017).

Acknowledgment

We would like to thank the patients and their families and all the investigators, including the physicians and laboratory technicians in this study.

Funding

This study was supported by the State Key Laboratory of Radiation Medicine and Protection (GZK1202106).

Conflict of Interest

The authors declare no conflict of interest.

References

[1] Johnson CA, James D, Marzan A, Armaos M. Cervical Cancer: An Overview of Pathophysiology and Management. Seminars in Oncology Nursing. 2019; 35: 166–174.

[2] Bruni L, Serrano B, Roura E, Alemany L, Cowan M, Herrero R, *et al*. Cervical cancer screening programmes and age-specific coverage estimates for 202 countries and territories worldwide: a review and synthetic analysis. The Lancet. Global Health. 2022; 10: e1115–e1127.

[3] Rahangdale L, Mungo C, O'Connor S, Chibwesha CJ, Brewer NT. Human papillomavirus vaccination and cervical cancer risk. British Medical Journal. 2022; 379: e070115.

[4] Pimple S, Mishra G. Cancer cervix: Epidemiology and disease burden. Cytojournal. 2022; 19: 21.

[5] Basoya S, Anjankar A. Cervical Cancer: Early Detection and Prevention in Reproductive Age Group. Cureus. 2022; 14: e31312.

[6] Sun Q, Wang L, Zhang C, Hong Z, Han Z. Cervical cancer heterogeneity: a constant battle against viruses and drugs. Biomarker Research. 2022; 10: 85.

[7] Banerjee D, Mittal S, Mandal R, Basu P. Screening technologies for cervical cancer: Overview. Cytojournal. 2022; 19: 23.

[8] Sivars L, Palsdottir K, Crona Guterstam Y, Falconer H, Hellman K, Tham E. The current status of cell-free human papillomavirus DNA as a biomarker in cervical cancer and other HPV-associated tumors: A review. International Journal of Cancer. 2023; 152: 2232–2242.

[9] Martínez-Rodríguez F, Limones-González JE, Mendoza-Almanza B, Esparza-Ibarra EL, Gallegos-Flores PI, Ayala-Luján JL, *et al*. Understanding Cervical Cancer through Proteomics. Cells. 2021; 10: 1854.

[10] Li JP, Kusche-Gullberg M. Heparan Sulfate: Biosynthesis, Structure, and Function. International Review of Cell and Molecular Biology. 2016; 325: 215–273.

[11] Sorrell JM, Caplan AI. Heparan Sulfate: A Regulator of White Adipocyte Differentiation and of Vascular/Adipocyte Interactions. Biomedicines. 2022; 10: 2115.

[12] Pretorius D, Richter RP, Anand T, Cardenas JC, Richter JR. Alterations in heparan sulfate proteoglycan synthesis and sulfation and the impact on vascular endothelial function. Matrix Biology Plus. 2022; 16: 100121.

[13] Cole CL, Rushton G, Jayson GC, Avizienyte E. Ovarian cancer cell heparan sulfate 6-O-sulfotransferases regulate an angiogenic program induced by heparin-binding epidermal growth factor (EGF)-like growth factor/EGF receptor signaling. The Journal of Biological Chemistry. 2014; 289: 10488–10501.

[14] Xu Y, Moon AF, Xu S, Krahn JM, Liu J, Pedersen LC. Structure Based Substrate Specificity Analysis of Heparan Sulfate 6-O-Sulfotransferases. ACS Chemical Biology. 2017; 12: 73–82.

[15] Howard SR, Oleari R, Poliandri A, Chantzara V, Fantin A, Ruiz-Babot G, *et al*. HS6ST1 Insufficiency Causes Self-Limited Delayed Puberty in Contrast With Other GnRH Deficiency Genes. The Journal of Clinical Endocrinology and Metabolism. 2018; 103: 3420–3429.

[16] Hu S, Xia C, Zou H, Ren W, Liu L, Wang L, *et al*. HS6ST1 overexpressed in cancer-associated fibroblast and inhibited cholangiocarcinoma progression. Digestive and Liver Disease. 2023; 55: 1114–1125.

[17] Iravani O, Bay BH, Yip GWC. Silencing HS6ST3 inhibits growth and progression of breast cancer cells through suppressing IGF1R and inducing XAF1. Experimental Cell Research. 2017; 350: 380–389.

[18] Zhang Y, Yu Y, Cao X, Chen P. Role of lncRNA FAM83H antisense RNA1 (FAM83H-AS1) in the progression of non-small cell lung cancer by regulating the miR-545-3p/heparan sulfate 6-O-sulfotransferase (HS6ST2) axis. Bioengineered. 2022; 13: 6476–6489.

[19] Jin Y, He J, Du J, Zhang RX, Yao HB, Shao QS. Overexpression of HS6ST2 is associated with poor prognosis in patients with gastric cancer. Oncology Letters. 2017; 14: 6191–6197.

[20] Hatabe S, Kimura H, Arao T, Kato H, Hayashi H, Nagai T, *et al*. Overexpression of heparan sulfate 6-*O*-sulfotransferase-2 in colorectal cancer. Molecular and Clinical Oncology. 2013; 1: 845–850.

[21] Vu M, Yu J, Awolude OA, Chuang L. Cervical cancer worldwide. Current Problems in Cancer. 2018; 42: 457–465.

[22] Habuchi H, Tanaka M, Habuchi O, Yoshida K, Suzuki H, Ban K, *et al*. The occurrence of three isoforms of heparan sulfate 6-O-sulfotransferase having different specificities for hexuronic acid adjacent to the targeted N-sulfoglucosamine. The Journal of Biological Chemistry. 2000; 275: 2859–2868.

[23] Habuchi H, Miyake G, Nogami K, Kuroiwa A, Matsuda Y, Kusche-Gullberg M, *et al*. Biosynthesis of heparan sulphate with diverse structures and functions: two alternatively spliced forms of human heparan sulphate 6-O-sulphotransferase-2 having different expression patterns and properties. The Biochemical Journal. 2003; 371: 131–142.

[24] Nagai N, Habuchi H, Esko JD, Kimata K. Stem domains of heparan sulfate 6-O-sulfotransferase are required for Golgi localization, oligomer formation and enzyme activity. Journal of Cell Science. 2004; 117: 3331–3341.

[25] Roldán FL, Izquierdo L, Ingelmo-Torres M, Lozano JJ, Carrasco R, Cuñado A, *et al*. Prognostic Gene Expression-Based Signature in Clear-Cell Renal Cell Carcinoma. Cancers. 2022; 14: 3754.

[26] Balasubramaniam SD, Balakrishnan V, Oon CE, Kaur G. Key Molecular Events in Cervical Cancer Development. Medicina. 2019; 55: 384.

[27] Nagai N, Habuchi H, Sugaya N, Nakamura M, Imamura T, Watanabe H, *et al*. Involvement of heparan sulfate 6-O-sulfation in the regulation of energy metabolism and the alteration of thyroid hormone levels in male mice. Glycobiology. 2013; 23: 980–992.

[28] Ushakov VS, Tsidulko AY, de La Bourdonnaye G, Kazanskaya GM, Volkov AM, Kiselev RS, *et al*. Heparan Sulfate Biosynthetic System Is Inhibited in Human Glioma Due to EXT1/2 and HS6ST1/2 Down-Regulation. International Journal of Molecular Sciences. 2017; 18: 2301.

[29] Gennigens C, Jerusalem G, Lapaille L, De Cuypere M, Streel S, Kridelka F, *et al*. Recurrent or primary metastatic cervical cancer: current and future treatments. ESMO Open. 2022; 7: 100579.

[30] Maiorano BA, Maiorano MFP, Ciardiello D, Maglione A, Orditura M, Lorusso D, *et al*. Beyond Platinum, ICIs in Metastatic Cervical Cancer: A Systematic Review. Cancers. 2022; 14: 5955.

[31] Lin CL, Ying TH, Yang SF, Chiou HL, Chen YS, Kao SH, *et al*. MTA2 silencing attenuates the metastatic potential of cervical cancer cells by inhibiting AP1-mediated MMP12 expression via the ASK1/MEK3/p38/YB1 axis. Cell Death & Disease. 2021; 12: 451.

[32] Li J, Liu C, Li D, Wan M, Zhang H, Zheng X, *et al*. OLFM4 Inhibits Epithelial-Mesenchymal Transition and Metastatic Potential of Cervical Cancer Cells. Oncology Research. 2019; 27: 763–771.

[33] Xing Q, Zeng T, Liu S, Cheng H, Ma L, Wang Y. A novel 10 glycolysis-related genes signature could predict overall survival for clear cell renal cell carcinoma. BMC Cancer. 2021; 21: 381.

[34] Tillo M, Charoy C, Schwarz Q, Maden CH, Davidson K, Fantin A, *et al*. 2- and 6-O-sulfated proteoglycans have distinct and complementary roles in cranial axon guidance and motor neuron migration. Development. 2016; 143: 1907–1913.

[35] Sepulveda-Diaz JE, Alavi Naini SM, Huynh MB, Ouidja MO, Yanicostas C, Chantepie S, *et al*. HS3ST2 expression is critical for the abnormal phosphorylation of tau in Alzheimer's disease-related tau pathology. Brain. 2015; 138: 1339–1354.